

ANS Binding Reveals Common Features of Cytotoxic Amyloid Species

Benedetta Bolognesi[†], Janet R. Kumita[†], Teresa P. Barros[†], Elin K. Esbjorner[†], Leila M. Luheshi[†], Damian C. Crowther[‡], Mark R. Wilson[§], Christopher M. Dobson[†], Giorgio Favrin^{*†¶}, and Justin J. Yerbury^{*†§}

[†]Department of Chemistry, University of Cambridge, Cambridge CB2 1EW, United Kingdom, [‡]Department of Genetics, University of Cambridge, Cambridge CB2 3EH, United Kingdom, [§]School of Biological Sciences, University of Wollongong, Wollongong 2522, Australia, and [¶]Department of Biochemistry, University of Cambridge, Cambridge CB2 1GA, United Kingdom

A large number of pathological conditions is now known to be associated with the deposition of normally soluble peptides and proteins as thread-like aggregates rich in β -sheet structure and known as amyloid fibrils (1). It is increasingly clear that the intrinsic ability to form such highly organized structures is not restricted to disease-associated peptides and proteins, but rather, is a generic property common to all polypeptide chains (2). The propensity to form amyloid fibrils and the proportion of fibrils relative to other aggregated species, is, however, highly variable as they are modulated by the composition and order of the side chains within individual sequences. Indeed, increasing evidence suggests that the small, heterogeneous, and soluble aggregates that often precede amyloid fibril formation (3) are responsible, at least in part, for the pathogenesis of the protein deposition diseases with which they are associated (4–9).

There is strong indication that intrinsic physicochemical properties, such as hydrophobicity and charge, influence the propensities of polypeptides to form both fibrils and the potentially much more pathogenic oligomeric species (10, 11). Moreover, recent work has shown remarkable correlations between the aggregation propensities of proteins, calculated from these intrinsic physicochemical properties, and their cyto-

toxicity. This appears to be the case both in transgenic models of neurodegeneration and in patients suffering from neurodegenerative diseases (12, 13). Importantly, it has also been found that of polypeptides not related to any known disease are not only able to aggregate further into amyloid fibrils but also to generate cytotoxic oligomeric species during the aggregation process (14–16). Moreover, common structural epitopes have been detected on prefibrillar aggregates made by a variety of polypeptides (17). These findings suggest that at least some common features exist in the mechanisms by which aggregates, formed by a great diversity of protein sequences, contribute to the pathogenesis of diseases associated with extracellular amyloid aggregation.

In light of the mounting evidence that toxic oligomers share structural similarities, it is of increasing importance to establish a link between the degree of toxicity and such features. To address this issue further, we have investigated the relationship between the cytotoxicity of species formed during amyloid aggregation and their biophysical properties.

RESULTS AND DISCUSSION

We first examined fibril formation by the E22G (arctic) variant of the 42-residue amyloid beta peptide ($A\beta_{1-42}$), which is

ABSTRACT Oligomeric assemblies formed from a variety of disease-associated peptides and proteins have been strongly associated with toxicity in many neurodegenerative conditions, such as Alzheimer's disease. The precise nature of the toxic agents, however, remains still to be established. We show that prefibrillar aggregates of E22G (arctic) variant of the $A\beta_{1-42}$ peptide bind strongly to 1-anilino-naphthalene 8-sulfonate and that changes in this property correlate significantly with changes in its cytotoxicity. Moreover, we show that this phenomenon is common to other amyloid systems, such as wild-type $A\beta_{1-42}$, the I59T variant of human lysozyme and an SH3 domain. These findings are consistent with a model in which the exposure of hydrophobic surfaces as a result of the aggregation of misfolded species is a crucial and common feature of these pathogenic species.

*Corresponding authors, gf247@cam.ac.uk and jyerbury@uow.edu.au.

Received for review January 27, 2010 and accepted June 15, 2010.

Published online June 15, 2010

10.1021/cb1001203

© 2010 American Chemical Society

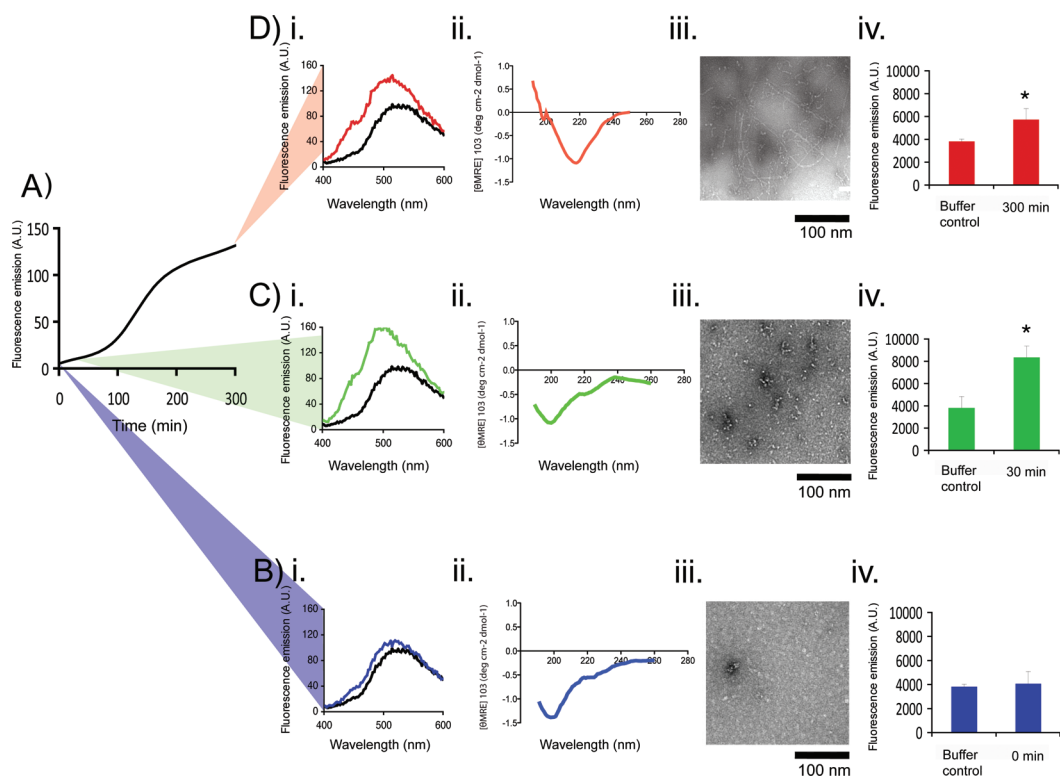


Figure 1. Biophysical characterization of the aggregation of E22G A β_{1-42} . The peptide was incubated in solution at 29 °C for 300 min. Aliquots were taken at various times for biophysical analysis. **A)** The progression of the aggregation was monitored by *ex situ* ThT fluorescence spectroscopy. The aggregates in the solutions were further characterized: **B)** prior to incubation, **C)** after 30 min, and **D)** 300 min of aggregation. We examined: **i)** ANS fluorescence spectrum (peptide is colored, buffer is black line), **ii)** Far UV CD spectrum, **iii)** TEM (scale bar = 100 nm), **iv)** cytotoxicity as measured by PI incorporation of SH-SY5Y cells to which control buffer and peptide were added. ThT and ANS fluorescence data are single measurements, CD data are the mean of four determinations and the PI fluorescence is the mean of triplicate determinations, and the error bars represent standard error of the mean. Significant differences ($p < 0.05$) from the control sample are indicated by *. All results shown are representative of at least seven independent experiments.

associated with an early onset inherited form of Alzheimer's disease (18). Although the method used to generate solutions of the peptide produces monomeric A β_{1-42} (see Supporting Information for details), transmission electron micrographs (TEMs) revealed that an overwhelmingly small number of nonfibrillar aggregates were already present upon initial TEM imaging (Figure 1, panel B, iii) demonstrating the considerable propensity of this peptide to aggregate. The circular dichroism (CD) spectrum of the same sample is random-coil like, with

a minimum at 200 nm (Figure 1, panel B, ii). Thirty minutes after dissolution, while the CD spectrum remains principally random coil-like (Figure 1, panel C, ii), a decrease in ellipticity at 215 nm indicates that the peptide molecules present are beginning to adopt an average conformation that is more β -sheet rich, a finding that is in accord with a simultaneous small increase in the fluorescence of the dye thioflavin T (ThT), (Figure 1, panel A), which exhibits a characteristic increase in quantum yield on interaction with ordered β -sheet structures (19).

binding hydrophobic patches, not present in the preceding monomers, but that these do not yet possess the long-range structural order characteristic of amyloid fibrils.

After *ca.* 300 min, not only has the ThT fluorescence reached its maximum intensity (Figure 1, panel A) but the CD spectrum of the sample is now characteristic of a predominantly β -sheet structure (Figure 1, panel D, ii). TEM images confirm that many fibrillar aggregates are now present, although a significant population of prefibrillar structures can still be observed. The

These changes take place at the same time as an increase in the size and abundance of 'worm-like' aggregates which can be visualized by TEM (Figure 1, panel C, iii). Even more strikingly, these are concomitant with a substantial increase in fluorescence intensity from 1-anilinonaphthalene 8-sulfonate (ANS), a dye whose spectral properties and quantum yield are highly sensitive to polarity and viscosity and, therefore, responds with an increase in intensity upon interaction with exposed hydrophobic regions in native or partially unfolded proteins (compare Figure 1, panels B and C, i) (20, 21). Although we cannot rule out the possibility that ANS binds to other structural features, our data collectively suggest that the E22G A β_{1-42} prefibrillar oligomeric species expose ANS-

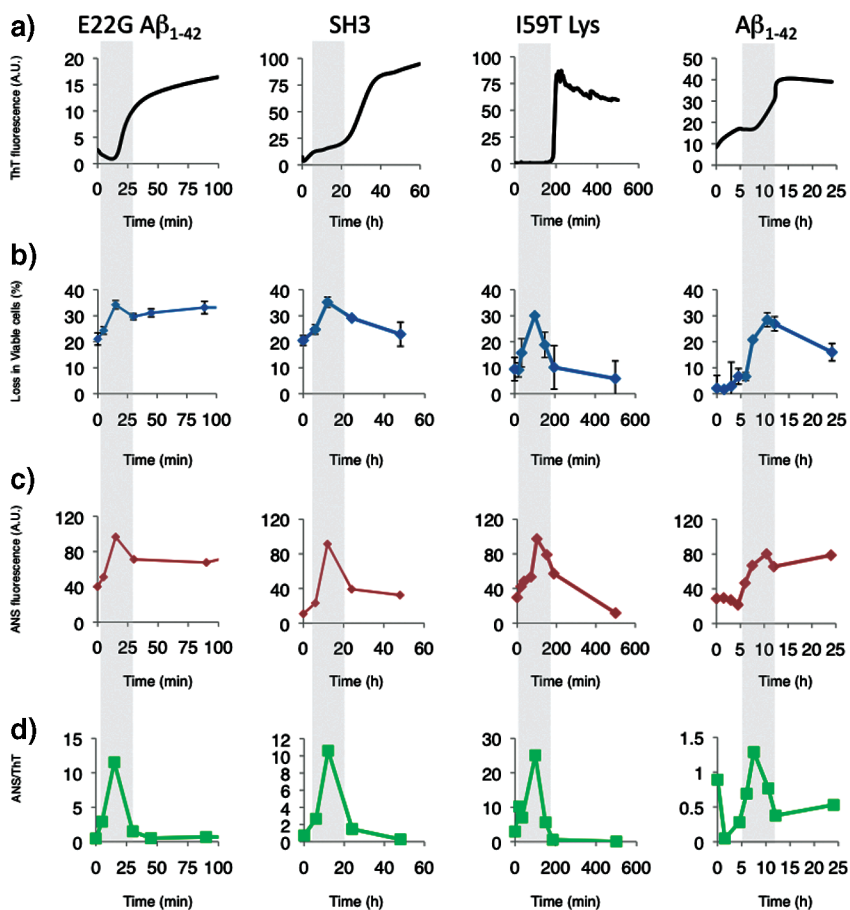


Figure 2. ANS binding and toxicity of early amyloid aggregates. Fluorescence and toxicity of the amyloid forming proteins E22G A β_{1-42} , SH3-PI3, I59T lysozyme, and A β_{1-42} . a) The progression of aggregation as monitored by ThT fluorescence. b) Toxicity of the aggregates as measured by PI uptake of SH-SY5Y cells to which aggregates taken at different time points were added. c) ANS fluorescence signal of aggregate solutions taken from different time points during aggregation. d) ANS/ThT ratio against time where the ratio is calculated using the absolute increment of both parameters. The columns refer to E22G A β_{1-42} (left), SH3-PI3 (middle-left), I59T lysozyme (middle-right), and A β_{1-42} (right). Data points in a) and c) are single measurements, while data points in b) are triplicate measurements with SE bars. All results shown for E22G A β_{1-42} , SH3-PI3, I59T lysozyme, and WT A β_{1-42} are representative of at least seven, three, three, and five independent experiments respectively.

sample taken at this time point possesses a substantial ANS fluorescence (Figure 1, panel D, i), consistent with the existence of a significant number of small heterogeneous aggregates with exposed hydrophobic surfaces remaining in solution alongside the more ordered fibrillar species that stimulate a lower level of ANS fluorescence

(Figure 1, panel D, iii; Supplementary Figure 1).

We next sought to understand the relationship between the changing structural characteristics of these E22G A β_{1-42} aggregates and their effects on the viability of neuronal cells. To achieve this objective, aliquots taken at different time points during

aggregation were added to cultures of SH-SY5Y human neuroblastoma cells, and the resulting changes in cell viability were measured by means of a propidium iodide (PI) incorporation assay and a Calcein AM assay. Addition of 1 μ M of an E22G A β_{1-42} aggregate solution resulted in increased PI staining of cell nuclei after 48 h of incubation. Using confocal microscopy, we found that the oligomeric aggregates bind almost immediately (within 5 min) to the cell surface and thus do not remain free in solution to continue the process of aggregation (Supplementary Figure 2). We further observed that increased PI fluorescence occurs concurrently with the increased ANS fluorescence intensity of the sample (compare Figure 1, panels B–D, iv) but not its ThT fluorescence. Fluorescence microscopy images revealed a high proportion of PI-stained cells in cultures treated with aliquots of E22G A β_{1-42} taken after 15 min of aggregation (Supplementary Figure 3). PI-stained cells were physically smaller and had partially lost their adherence properties and exhibited retracted processes typical of dead or dying SH-SY5Y cells (Supplementary Figure 3). Furthermore, cells treated with aliquots taken at 300 min, which showed a high ANS signal and was observed by TEM to contain abundant prefibrillar species, showed similar changes. Indeed, a more thorough analysis of E22G A β_{1-42} aggregation shows that there is a peak in the ANS fluorescence prior to a substantial increase in that of ThT. This peak in ANS fluorescence corresponds closely to a peak in toxicity of the aggregates (Figure 2, panel b), and the correlation between ANS fluorescence intensity and toxicity (measured by both dead cells and cell viability assays) is statistically significant (Figure 3, panel a and Supplementary Figure 4, $R^2 = 0.85$ $p < 0.01$ and $R^2 = 0.71$ $p < 0.01$). This result suggests that the most cytotoxic types of aggregates formed by E22G A β_{1-42} are the prefibrillar species present during the lag phase that interact more strongly with ANS. Moreover, the toxic-

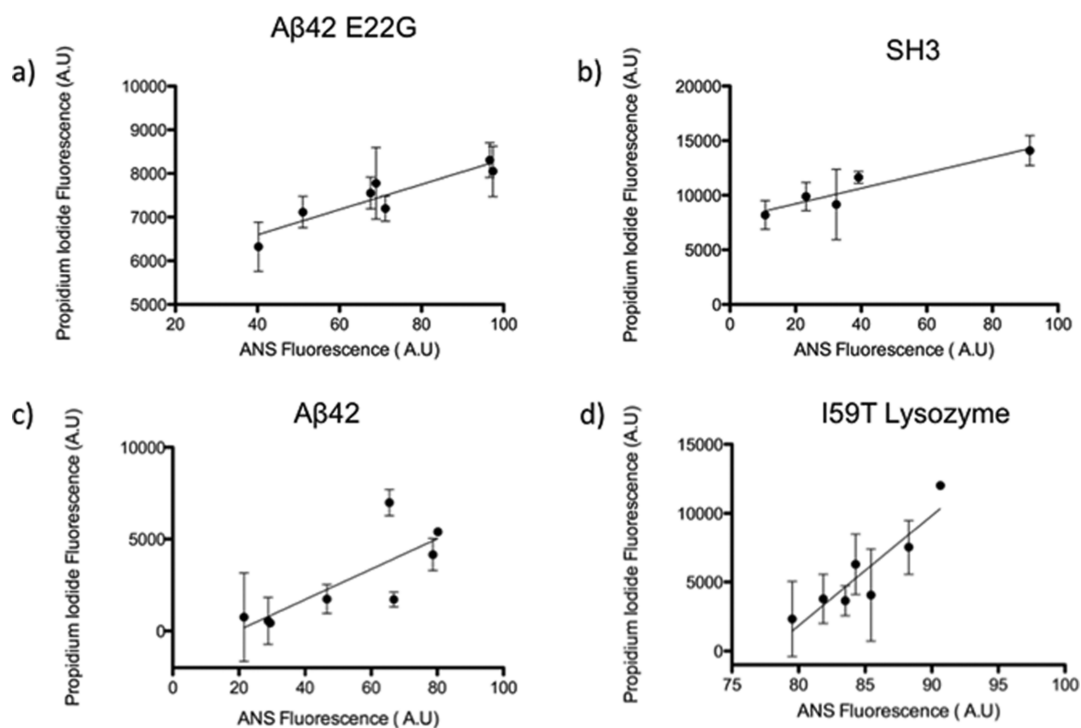


Figure 3. Correlation of ANS binding of aggregates with toxicity. Correlation graphs of the increment in ANS fluorescence signal and the corresponding increment in toxicity, as measured by PI incorporation, of the aggregates at different time points for a) E22G A β_{1-42} , b) PI3-SH3, c) I59T lysozyme, and d) WT A β_{1-42} . ANS data points are single measurements, while PI fluorescence data points are the mean of three measurements. Error bars represent standard error of the mean. The results shown for E22G A β_{1-42} , SH3-PI3, I59T lysozyme, and A β_{1-42} are representative of at least seven, three, three, and five independent experiments respectively.

ity persists even after mature fibrils are formed, either because of the persistence or regeneration of oligomeric species (as indicated in Supplementary Figure 1) or from a degree of intrinsic toxicity of the fibrillar material (12, 22).

In light of the correlation between the toxicity and the ANS fluorescence intensity in samples of E22G A β_{1-42} aggregates, we carried out analogous experiments with three further amyloidogenic peptides and proteins, namely wild-type A β_{1-42} , the I59T variant of lysozyme (23), and the SH3 domain of PI3 kinase (24). We found equally striking correlations in these systems between the increase in ANS fluorescence in samples taken at various time points during aggregation and their toxicity (Figure 2 and Figure 3: $R^2 = 0.62$, $p < 0.05$; $R^2 = 0.82$, $p < 0.01$;

and $R^2 = 0.89$, $p < 0.01$, respectively). In all cases the ratio of the ANS to ThT fluorescence of the different systems shows a dramatic increase during the lag phase before ThT-binding amyloid fibrils are formed (Figure 2, panel d). Moreover, this increase in the fluorescence ratio appears as the toxicity of the samples is at its greatest (Figure 2, panel b). Except for the case of A β_{1-42} , for which the time course of the development of ANS and ThT fluorescence is rather similar, it can be seen clearly that the ThT fluorescence intensity does not correlate with ANS binding or with toxicity for the different peptides and proteins studied in this work (Supplementary Figure 5).

Our data support earlier evidence (4–7) that prefibrillar aggregates are the most toxic amyloid-related species but in addi-

tion link a characteristic, namely ANS binding, to the toxicity of these aggregates regardless of the protein or peptide from which they are formed. As ANS is widely used to measure exposed hydrophobic patches on proteins, (20, 21) the data suggest that the presence of exposed hydrophobic patches is a common feature of highly toxic soluble aggregates. We cannot, however, exclude the possibility that ANS is binding to an alternative common structural feature of prefibrillar aggregates or that another structural feature, such as physical size, appearing concomitant to ANS binding plays an important role in aggregate toxicity (25). It has been shown, however, that oligomers of the same protein and of approximately the same physical size can possess very different degrees of toxicity and levels of exposed hydrophobicity (26, 27). Our data supports these observations and in addition suggests that there is a general correlation between these two characteristics.

Our data showing that the toxicity of aggregates formed from a range of polypeptides correlates with their increased fluorescence in the presence of ANS are also in accord with a “coalescence and reorganization” model of amyloid formation (28, 29). This model proposes that, after an initial hydrophobic collapse, the generation of a more stable hydrogen-bonded core drives the exposure of the hydrophobic residues

that were buried in the initial collapse. This process results, initially, in many soluble, hydrophobic aggregates with a high surface-to-volume ratio and is consistent with our observations. Such aggregates are likely to have an ability to bind rapidly and nonspecifically to cell surfaces, a potential first step in generating a toxic response. Previous results (28, 30) indicate that as aggregates increase in size over time, their surface-to-volume ratio decreases. Consequently the overall exposed hydrophobicity of the system will be reduced, as is shown most dramatically in the cases of SH3 and I59T lysozyme.

Although the present results indicate the existence of a common feature that is associated with the toxicity of aggregates formed by a number of peptides and proteins, as with other common features of the generic amyloid phenomenon (1), the amino acid sequence plays an important role in defining the specific properties of these aggregates. In all of the systems studied here, the increment in ANS fluorescence intensity correlates linearly with the increase in toxicity; the slope of this linear relationship is, however, sequence dependent (Figure 3). Apart from the obvious differences in the content of hydrophobic amino acid residues of the different systems, variations in the polypeptide sequences influence other properties, such as the stability of the native state, the intrinsic propensity to aggregate, the distinct nature of the residues exposed during aggregation, and both the size and relative population of aggregates. The specific degree of toxicity of each protein is, therefore, likely to be influenced not only by the number of hydrophobic side chains that these oligomers expose but also by their relative ability to form such oligomers and the relative rates at which they convert into mature fibrillar species.

Any increase in hydrophobicity, however, is likely to promote the rapid and nonspecific binding of aggregates to cell membranes (Supplementary Figure 2) where they

have been shown to interact with cell surface receptors leading to changes in the transduction of intracellular signaling cascades potentially leading to the degeneration of the cell (6). Alternatively, it is possible that hydrophobic aggregates can insert into, and then interfere directly with, membrane structure resulting in changes in membrane permeability and subsequent toxicity (31–33). The precise interactions which trigger this chain of events, may depend on the location of the aggregating protein *in vivo* as well as the repertoire of accessible membrane-bound proteins, providing a rationale for disease specificity. In conclusion, our results not only provide direct evidence for a common step in the mechanism by which toxicity of polypeptide oligomers emerges but also strongly support the proposition that the exposure of hydrophobic patches is a key feature of the toxicity of extracellular oligomeric species.

METHODS

Peptides and Proteins. A β_{1-42} and E22G A β_{1-42} , synthesized through solid-phase synthesis, were purchased from Bachem. Solutions of the peptides were prepared by a TFA/HFIP dissolution method which disrupts preformed aggregates initially present (34). I59T human lysozyme was recombinantly expressed in *P. pastoris* and purified as previously described (35). SH3-PI3 was expressed in *E. coli* and purified as described (36). Further details are provided in the Supporting Information.

ANS Fluorescence. Aliquots of the peptide or protein solutions under aggregating conditions were taken at the time points indicated and diluted to give a 10 μ M concentration in 200 mM ANS and 50 mM NaH₂PO₄. A Cary Eclipse Fluorimeter (Varian Ltd.) was used to record fluorescence spectra between 400 and 600 nm upon excitation of the sample at 350 nm.

Cell Culture. SH-SY5Y cells were cultured in Dulbecco's Modified Eagle Medium (Invitrogen) with the addition of 10% fetal bovine serum at 37 °C in a humidified 5% CO₂ incubator. The cells were plated in Costar (3595) 96-well plates (Corning) using serum-free Neurobasal medium (GIBCO) and were then incubated with 1 μ M aggregates for 48 h. The percentage of dead cells present after 48 h was assessed by adding PI to the cell culture medium and measuring the fluorescence emitted by the PI-stained nuclei of dead cells using a FLUOstar OPTIMA plate reader (BMG LabTech). Alternatively, after 48 h, the percentage of live cells was assessed by adding Calcein AM and measur-

ing fluorescence of calcein, the product of its hydrolyzation by intracellular esterases.

Details on: Peptide and protein preparation, protein aggregation and ThT fluorescence, sample preparation for transmission electron microscopy and cell imaging are all given in the Supporting Information.

Acknowledgment: Our work has been supported by the Alzheimer's Research Trust (B.B., D.C.C., and C.M.D.), the MRC (D.C.C. and C.M.D.), the EPSRC (G.F.), and the ARC (J.J.Y.).

Supporting Information Available: This material is available free of charge via the Internet at <http://pubs.acs.org>.

REFERENCES

- Chiti, F., and Dobson, C. M. (2006) Protein misfolding, functional amyloid, and human disease, *Annu. Rev. Biochem.* **75**, 333–66.
- Dobson, C. M. (1999) Protein misfolding, evolution and disease, *Trends Biochem. Sci.* **24**, 329–32.
- Calamai, M., Chiti, F., and Dobson, C. M. (2005) Amyloid fibril formation can proceed from different conformations of a partially unfolded protein, *Bio-phys. J.* **89**, 4201–10.
- Cleary, J. P., Walsh, D. M., Hofmeister, J. J., Shankar, G. M., Kuskowski, M. A., Selkoe, D. J., and Ashe, K. H. (2005) Natural oligomers of the amyloid-beta protein specifically disrupt cognitive function, *Nat. Neurosci.* **8**, 79–84.
- Ferreira, S. T., Vieira, M. N., and De Felice, F. G. (2007) Soluble protein oligomers as emerging toxins in Alzheimer's and other amyloid diseases, *IUBMB Life* **59**, 332–45.
- Li, S., Hong, S., Sheppardson, N. E., Walsh, D. M., Shankar, G. M., and Selkoe, D. (2009) Soluble oligomers of amyloid Beta protein facilitate hippocampal long-term depression by disrupting neuronal glutamate uptake, *Neuron* **62**, 788–801.
- Selkoe, D. J. (2008) Soluble oligomers of the amyloid beta-protein impair synaptic plasticity and behavior, *Behav. Brain Res.* **192**, 106–13.
- Karpinar, D. P., Balija, M. G. G., Kögler, S., Opazo, F., Rezaei-Ghaleh, N., Wender, N., Kim, H. Y., Taschenberger, G., Falkenburger, G. H., and Heise, H., *et al.* (2009) Pre-fibrillar α -synuclein variants with impaired β -structure increase neurotoxicity in Parkinson's disease models, *EMBO J.* **28**, 3256–3268.
- Carrell, R. W., Mushunje, A., and Zhou, A. (2008) Serpins show structural basis for oligomer toxicity and amyloid ubiquity, *FEBS Lett.* **582**, 2537–2541.
- Chiti, F., Taddei, N., Baroni, F., Capanni, C., Stefani, M., Ramponi, G., and Dobson, C. M. (2002) Kinetic partitioning of protein folding and aggregation, *Nat. Struct. Biol.* **9**, 137–43.
- Pawar, A. P., Dubay, K. F., Zurdo, J., Chiti, F., Vendruscolo, M., and Dobson, C. M. (2005) Prediction of "aggregation-prone" and "aggregation-susceptible" regions in proteins associated with neurodegenerative diseases, *J. Mol. Biol.* **350**, 379–92.
- Luheshi, L. M., Tartaglia, G. G., Brorsson, A. C., Pawar, A. P., Watson, I. E., Chiti, F., Vendruscolo, M., Lomas, D. A., Dobson, C. M., and Crowther, D. C. (2007) Systematic *in vivo* analysis of the intrinsic determinants of amyloid Beta pathogenicity, *PLoS Biol.* **5**, e290.

13. Wang, Q., Johnson, J. L., Agar, N. Y., and Agar, J. N. (2008) Protein aggregation and protein instability govern familial amyotrophic lateral sclerosis patient survival, *PLoS Biol.* 6, e170.
14. Bucciantini, M., Calloni, G., Chiti, F., Formigli, L., Nosi, D., Dobson, C. M., and Stefani, M. (2004) Prefibrillar amyloid protein aggregates share common features of cytotoxicity, *J. Biol. Chem.* 279, 31374–82.
15. Bucciantini, M., Giannoni, E., Chiti, F., Baroni, F., Formigli, L., Zurdo, J., Taddei, N., Ramponi, G., Dobson, C. M., and Stefani, M. (2002) Inherent toxicity of aggregates implies a common mechanism for protein misfolding diseases, *Nature* 416, 507–11.
16. Morozova-Roche, L. A. (2007) Equine lysozyme: the molecular basis of folding, self-assembly and innate amyloid toxicity, *FEBS Lett.* 581, 2587–92.
17. Kaye, R., Head, E., Thompson, J. L., McIntire, T. M., Milton, S. C., Cotman, C. W., and Glabe, C. G. (2003) Common structure of soluble amyloid oligomers implies common mechanism of pathogenesis, *Science* 300, 486–9.
18. Lannfelt, L., Bogdanovic, N., Appelgren, H., Axelman, K., Lilius, L., Hansson, G., Schenk, D., Hardy, J., and Winblad, B. (1994) Amyloid precursor protein mutation causes Alzheimer's disease in a Swedish family, *Neurosci. Lett.* 168, 254–6.
19. Levine, H. (1999) Quantification of beta-sheet amyloid fibril structures with thioflavin T, *Methods Enzymol.* 309, 274–84.
20. Hawe, A., Sutter, M., and Jiskoot, W. (2008) Extrinsic fluorescent dyes as tools for protein characterization, *Pharm. Res.* 25, (7), 1487–99.
21. Matthews, C. R. (1993) Pathways of protein folding, *Annu. Rev. Biochem.* 62, 653–83.
22. Nilsberth, C., Westlind-Danielsson, A., Eckman, C. B., Condron, M. M., Axelman, K., Forsell, C., Stenh, C., Luthman, J., Teplow, D. B., Younkin, S. G., Naslund, J., and Lannfelt, L. (2001) The 'Arctic' APP mutation (E693G) causes Alzheimer's disease by enhanced Abeta protofibril formation, *Nat. Neurosci.* 4, 887–93.
23. Kumita, J. R., Poon, S., Caddy, G. L., Hagan, C. L., Dumoulin, M., Yerbury, J. J., Stewart, E. M., Robinson, C. V., Wilson, M. R., and Dobson, C. M. (2007) The extracellular chaperone clusterin potently inhibits human lysozyme amyloid formation by interacting with prefibrillar species, *J. Mol. Biol.* 369, 157–67.
24. Guijarro, J. I., Sunde, M., Jones, J. A., Campbell, I. D., and Dobson, C. M. (1998) Amyloid fibril formation by an SH3 domain, *Proc. Natl. Acad. Sci. U.S.A.* 95, 4224–8.
25. Xue, W. F., Hellewell, A. L., Hewitt, E. W., and Radford, S. E. (2010) Fibril fragmentation in amyloid assembly and cytotoxicity: When size matters, *Prion* 29, (1), 4.
26. Campioni, S., Mannini, B., Zampagni, M., Pensalfini, A., Parrini, C., Evangelisti, E., Relini, A., Stefani, M., Dobson, C. M., Cecchi, C., and Chiti, F. (2010) A causative link between the structure of aberrant protein oligomers and their ability to cause cellular dysfunction, *Nat. Chem. Biol.* 6, 140–7.
27. Frare, E., Mossuto, M. F., de Laureto, P. P., Tolin, S., Menzer, L., Dumoulin, M., Dobson, C. M., and Fontana, A. (2009) Characterization of oligomeric species on the aggregation pathway of human lysozyme, *J. Mol. Biol.* 287, 17–27.
28. Cheon, M., Chang, I., Mohanty, S., Luheshi, L. M., Dobson, C. M., Vendruscolo, M., and Favrin, G. (2007) Structural reorganisation and potential toxicity of oligomeric species formed during the assembly of amyloid fibrils, *PLoS Comput. Biol.* 3, 1727–38.
29. Serio, T. R., Cashikar, A. G., Kowal, A. S., Sawicki, G. J., Moslehi, J. J., Serpell, L., Amsdorf, M. F., and Lindquist, S. L. (2000) Nucleated conformational conversion and the replication of conformational information by a prion determinant, *Science* 289, 1317–21.
30. Kremer, J. J., Pallitto, M. M., Sklansky, D. J., and Murphy, R. M. (2000) Correlation of beta-amyloid aggregate size and hydrophobicity with decreased bilayer fluidity of model membranes, *Biochemistry* 39, 10309–10318.
31. Glabe, C. G. (2006) Common mechanisms of amyloid oligomer pathogenesis in degenerative disease, *Neurobiol. Aging* 27, 570–5.
32. Glabe, C. G. (2008) Structural classification of toxic amyloid oligomers, *J. Biol. Chem.* 283, 29639–43.
33. Kourie, J. I., and Henry, C. L. (2002) Ion channel formation and membrane-linked pathologies of misfolded hydrophobic proteins: the role of dangerous unchaperoned molecules, *Clin. Exp. Pharmacol. Physiol.* 29, 741–53.
34. Teplow, D. B. (2006) Preparation of amyloid beta-protein for structural and functional studies, *Methods Enzymol.* 413, 20–33.
35. Kumita, J. R., Johnson, R. J., Alcocer, M. J., Dumoulin, M., Holmqvist, F., McCammon, M. G., Robinson, C. V., Archer, D. B., and Dobson, C. M. (2006) Impact of the native-state stability of human lysozyme variants on protein secretion by *Pichia pastoris*, *FEBS J.* 273, 711–20.
36. Yerbury, J. J., Poon, S., Meehan, S., Thompson, B., Kumita, J. R., Dobson, C. M., and Wilson, M. R. (2007) The extracellular chaperone clusterin influences amyloid formation and toxicity by interacting with prefibrillar structures, *FASEB J.* 21, 2312–22.